Long-term stability of molecular doped epigraphene quantum Hall standards: single elements and large arrays (R K/236 ≈ 109 Ω)

(article starts on next page)

PAPER • OPEN ACCESS

Long-term stability of molecular doped epigraphene quantum Hall standards: single elements and large arrays ($R_K/236 \approx 109$ Ω)

View the article online for updates and enhancements.

Long-term stability of molecular doped epigraphene quantum Hall standards: single elements and large arrays ($R_K/236 \approx 109\ \Omega$)

Naveen Shetty[1] **, Tobias Bergsten**[2] **, Gunnar Eklund**[2]**, Samuel Lara Avila**[1,3]**, Sergey Kubatkin**[1]**, Karin Cedergren**[2] **and Hans He**[1,2,*]

[1] Department of Microtechnology and Nanoscience, Chalmers University of Technology, 412 96 Gothenburg, Sweden
[2] RISE Research Institutes of Sweden, Box 857, S-50115 Borås, Sweden
[3] National Physical Laboratory, Hampton Road, Teddington TW11 0LW, United Kingdom

E-mail: hans.he@rise.se

CrossMark

Abstract

In this work we investigate the long-term stability of epitaxial graphene (epigraphene) quantum Hall resistance standards, including single devices and an array device composed of 236 elements providing $R_K/236 \approx 109\ \Omega$, with R_K the von Klitzing constant. All devices utilize the established technique of chemical doping via molecular dopants to achieve homogenous doping and control over carrier density. However, optimal storage conditions and the long-term stability of molecular dopants for metrological applications have not been widely studied. In this work we aim to identify simple storage techniques that use readily available and cost-effective materials which provide long-term stability for devices without the need for advanced laboratory equipment. The devices are stored in glass bottles with four different environments: ambient, oxygen absorber, silica gel desiccant, and oxygen absorber/desiccant mixture. We have tracked the carrier densities, mobilities, and quantization accuracies of eight different epigraphene quantum Hall chips for over two years. We observe the highest stability (i.e. lowest change in carrier density) for samples stored in oxygen absorber/desiccant mixture, with a relative change in carrier density below 0.01% per day and no discernable degradation of quantization accuracy at the part-per-billion level. This storage technique yields a comparable stability to the currently established best storage method of inert nitrogen atmosphere, but it is much easier to realize in practice. It is possible to further optimize the mixture of oxygen absorber/desiccant for even greater stability performance in the future. We foresee that this technique can allow for simple and stable long-term storage of polymer-encapsulated molecular doped epigraphene quantum Hall standards, removing another barrier for their wide-spread use in practical metrology.

---

* Author to whom any correspondence should be addressed.

1. Introduction

Quantum Hall resistance standards (QHRs) made using epitaxial graphene (epigraphene) have been established as one of the most accurate primary resistance standards available [1–6]. The unique electronic nature of graphene [7], and epigraphene especially [8], has allowed for the creation of accurate QHRs with more relaxed operating conditions [2, 9] and more robust quantization plateaus [10]. Epigraphene-based QHRs have therefore started to slowly supplant the conventional QHRs made from GaAs-based materials in National Metrology Institutes (NMI) around the world.

However, there is one aspect where the conventional materials still have an advantage: long-term stability. GaAs-based QHRs can be kept in ambient conditions (e.g. in the desk drawer) for decades and still retain their original performance. For instance, the GaAs device at RISE comes from PTB and has been in use for routine resistance traceability since 1999, and was latest used in a comparison measurement in 2019 [11]. When not in use, this GaAs sample is just kept in ambient conditions.

The 2D-nature of graphene makes its resistance very sensitive to adsorbates, and to achieve long-term stability, graphene devices require passivation layers. For instance, ambient dopants can have a large influence on the carrier density [12], causing undesired drift over time if graphene is left unprotected. This is problematic because carrier density control of graphene is crucial to tune the operating conditions for quantum resistance metrology [2, 9]. We demonstrated a technique which yields potent and uniform doping of epigraphene by using molecular dopants and polymer encapsulation [11, 13, 14], and it allows an epigraphene QHR device to be tuned to operate at some desired temperature T, magnetic flux density B, and with critical current I_C. It has previously been demonstrated that the molecular dopant technique yields long-term stable doping if the samples are kept in inert nitrogen atmosphere, with a relative change in carrier density around 0.02% per day [11]. However, continuous access to nitrogen gas can be restrictive, and other simpler storage methods are desirable. Recent reports demonstrate alternative methods for molecular-doped epigraphene such as glass-encapsulation schemes with relative change in carrier density within 0.4%–0.5% per day [15]. While it offers a simple and permanent encapsulation scheme, these have yet to reach the same long-term stability as storage in inert nitrogen atmosphere.

2. Storage techniques

In this work we propose a simple approach to preserve epigraphene samples, which is available to practically every laboratory who desires to use epigraphene QHRs: sealed 100 ml glass bottles and food-grade chemicals. Glass bottles are made of borosilicate 3.3, from VWR® (with protective plastic coating). They are mounted with polypropylene (PP) pouring rings and a PP screw cap. We set up four different storage environments (see figure 1). The first storage method is an open glass bottle (no lid) which represents ambient atmosphere. The second method uses commercially available traditional silica gel (porous silicon dioxide) desiccant 1–3 mm beads, containing 98% SiO_2 and 2% mixture of Al_2O_3, TiO_2, Fe_2O_3. The silica creates a dry environment by moisture adsorption onto the surface of pores of gel beads, and they are rated at 250 g kg^{-1} water absorbing capacity (20 °C). Al_2O_3, TiO_2, Fe_2O_3 mixture helps to quantify the adsorption of H_2O, indicated by color change from orange to colorless. We used approximately 40 ml desiccant in the bottle. The third method utilizes a commercially available oxygen absorber from O2ZERO™, containing a mixture of ferrous iron powder (55%), silicon dioxide hydrate (25%), water (15%) and sodium chloride (5%). Ferrous iron oxide is converted to its activated ferric state; hydrated iron oxide after absorbing residual oxygen within the container, which creates an oxygen-poor environment [16]. Each oxygen absorber sachet is rated at 100 CC with 3.3 g gross weight, and we use three of them. The final method uses a mixture of desiccant and oxygen absorber, with approximately 30 ml desiccant and three oxygen absorber sachets.

Note that throughout this experiment we did not replace or refresh the contents of the bottles. The initial batch of desiccant pellets and oxygen absorber sachets remain inside the bottles from beginning to end.

3. Sample preparation

We tested in total eight molecularly-doped epigraphene QHRs: four produced on graphene grown on high purity semi-insulating SiC (HPSI, Cree), and four on semi-insulating compensated SiC (Atecom). Aside from this difference, all chips were fabricated into identical devices, with the same Hall bar geometries and doped using the same molecular doping technique. The details of the sample fabrication follow the instructions detailed in other works [11, 13]. One key difference in this work is that we utilize a new method to fabricate the Ti/Au-graphene edge contacts, which ensures low contact resistance to graphene [17].

After chemical doping, we used additional thermal annealing at 160 °C to tune all carrier densities to around 1–2 cm^{-2} × 10^{11} cm^{-2} (n-type). This carrier density level is ideal for precision measurements operating within our typical parameters of $T = 2$ K, $B = 5$ T, $I = 23$ μA [9]. For Cree substrates the additional annealing took around 30 min, while for Atecom it took more than 60 min. The difference in annealing
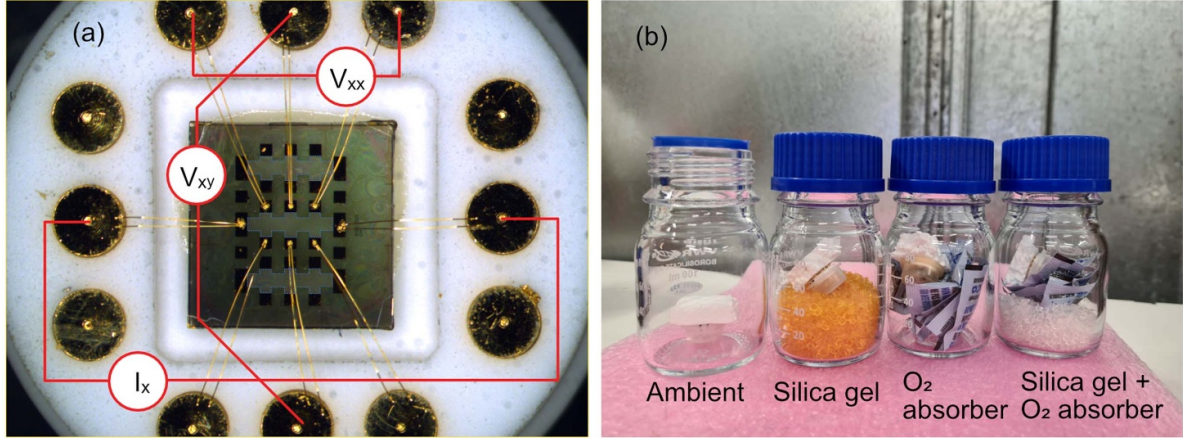
Figure 1. (a) Optical image of an epigraphene QHR chip (7 mm^2 × 7 mm^2), with three Hall bar devices. The chip is glued to a TO-8 holder, and the center Hall bar is wire bonded to the holder using Al/Si wires. (b) Photo of four glass bottles, and their respective storage environment. Each glass bottle holds one epigraphene QHR chip mounted on a TO-8 holder with a plastic lid.
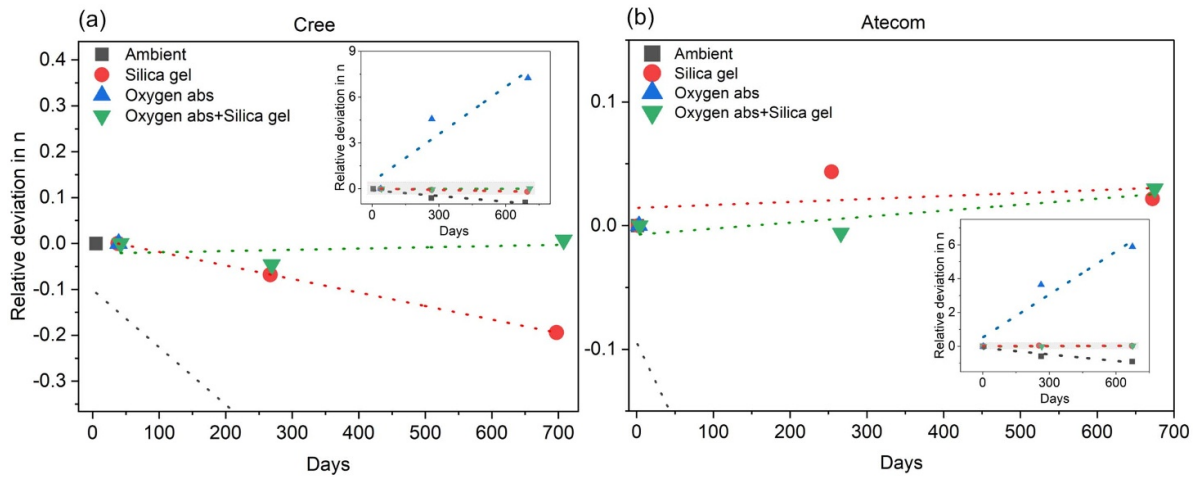

Figure 2. Measure of relative deviation in carrier concentration '*n*' of chemically doped epitaxial graphene samples kept in different storage environments over a period of two years. (a) is the zoomed in (shaded) part of inset in the top right corner for the Cree sample. In the mixture of oxygen absorber and silica gel environment sample shows high stability over the period of 700 d compared to other storage methods. (b) is the zoomed in (shaded) part of inset in the bottom right corner for the Atecom sample. Sample shows good stability not only in the mixture of oxygen absorber and silica gel environment, but also in the silica gel environment alone. Error bars are not included in the plot since the size of the data markers are of the order of one standard deviation.

time is attributed to different substrate-induced doping. All four storage types were tested for each substrate type, making in total eight devices spread across eight bottles.

4. Stability comparison

As the main indicator of stability, we use the relative change of carrier density *n* over time *t*, expressed as $(n(t) - n_0)/n_0$ where n_0 is the initial carrier density and $n(t)$ is the carrier density at a certain time. The carrier density was determined by measuring the Hall voltage V_{XY} while sweeping magnetic flux density *B* using 0.1 T steps. A linear regression fit is taken in the low-field linear regime to calculate the Hall coefficient R_H (the slope, unit Ω/T). The carrier density is then calculated as $n = 1/(eR_H)$, where *e* is elementary charge. The Hall

measurements were performed at temperature $T = 2$ K with a bias current $I = 23$ µA in a dry cryostat (Teslatron).

Figure 2 shows the summary of carrier density measurements performed for all samples, spanning a period of roughly 700 d.

After extended storage the carrier densities for samples kept in ambient or oxygen absorber have changed drastically. They are already too low ($\sim 10^{10}$ cm^{-2}) or too high ($\sim 10^{12}$ cm^{-2}) for proper quantization in typical operating conditions of 2 K, 5 T, and 23 µA bias. This means that these storage techniques are not suitable for long-term storage.

The samples kept in silica gel show signs of drift, especially for the Cree sample. While the drift can be significant, the samples can still be used for precision measurements in our typical operating conditions for a prolonged time. For the Atecom sample, the overall drift appears to be low, but the
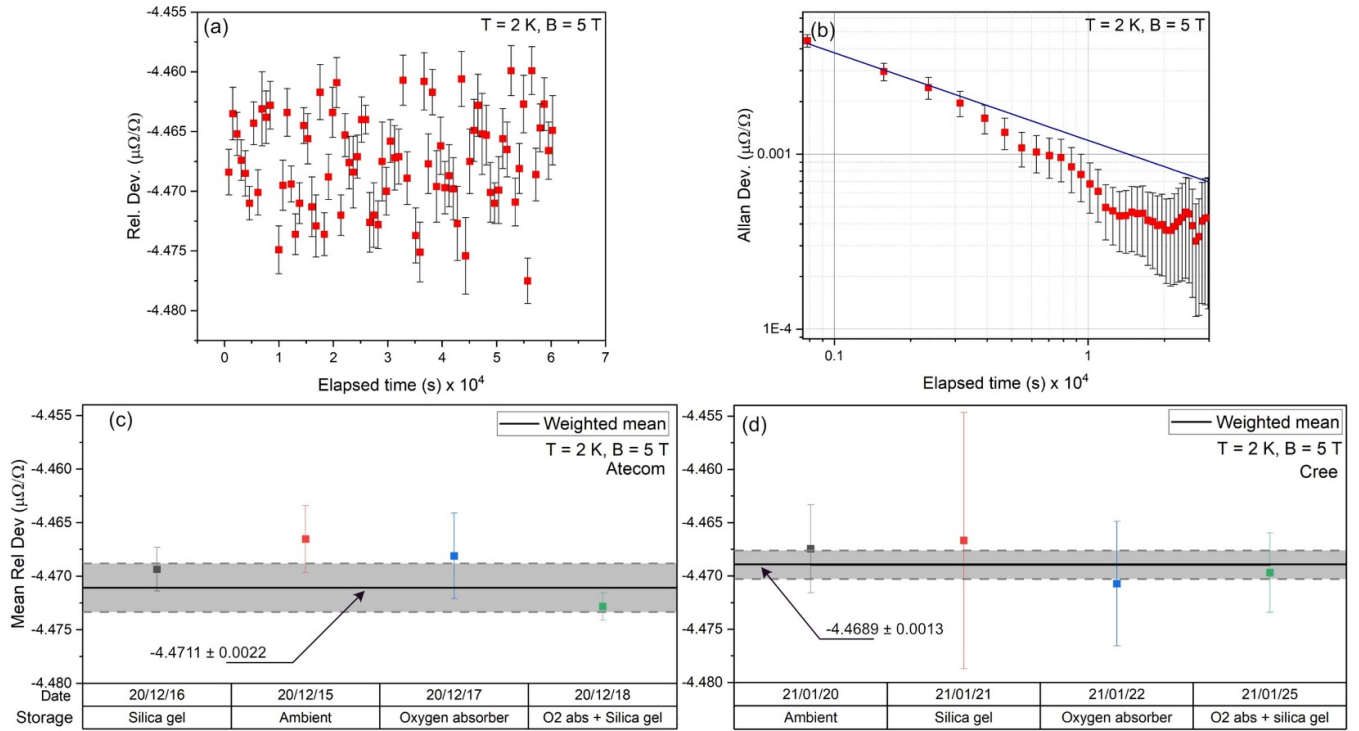
Figure 3. (a) One of the precision cryogenic current comparator (CCC) measurement of chemically doped epigraphene samples kept in ambient versus standard resistor with nominal value of 100 Ω, which shows the relative deviation of the 100 Ω standard from its nominal value at $B = 5$ T and $T = 2$ K. (b) Allan deviation follows $1/t^{1/2}$ (blue line), where t is the elapsed time, which indicates that white noise dominates down to below 1 nΩ Ω^{-1}. (c) and (d) are the precision measurements taken for samples kept in different environments shows the mean relative deviation between each sample and the 100 Ω standard resistor. Each point in (c) and (d) is the mean of over 60 CCC-series (like those in a), and error bars represent the standard type A uncertainty, derived from Allan deviation (like (b)) at 10^4 s for each measurement. The grey shaded area is the one standard deviation from the weighted mean (black line) of all data points.

variance between the measurements is very high, indicating some instability. Combined with the clear drift in the Cree case, the silica gel storage is serviceable, but non-ideal.

The most stable storage solution is the mixture of oxygen absorber and desiccant. In both cases, the drift appears to be low, with a slow increase in n-doping over time. The relative change in the carrier density per day is within (0.0027 ± 0.0082) % for Cree and within (0.0048 ± 0.0029) % for Atecom. All errors in this work are given with coverage factor one ($k = 1$) unless stated otherwise. The degree of stability compares favorably to the current best method of storage in nitrogen environment, which has a relative drift of 0.02% per day [11].

5. Initial precision measurements

Additionally, we complement the simple Hall measurements with precision comparison measurements between epigraphene QHRs in quantized regime with an established conventional resistance standard, to verify that the quantization accuracy is maintained over time. Prior to precision measurements, each Hall bar has been characterized in accordance with established guidelines [18]. Contact resistances were measured using 3-probe configuration and were all below 2 Ω (this

value includes the lead resistance of around 1.5 Ω) [17–19]. Longitudinal resistance R_{XX} was measured using a nanovoltmeter setup, and was limited to a noise floor of 100 nV, leading to a R_{XX} below 0.1 mΩ at least. For precision comparison measurements we utilize a cryogenic current comparator (CCC) to compare epigraphene QHRs (measured at 2 K, in dry cryostat Teslatron) with an established conventional 100 Ω (Tinsley make). The 100 Ω standard has a well-known history, with decades of data against various QHRs, and is extremely stable short term (standard deviation below 10 nΩ Ω^{-1}, noise can be averaged down to 1 nΩ Ω^{-1}), with a well-characterized slow long-term linear drift (relative change of nominal value less than 2 nΩ Ω^{-1} per 100 d). We utilize this 100 Ω to indirectly compare the epigraphene QHRs to each other. All CCC-measurement use a bias current of $I = 23$ μA for the QHRs, and 3 mA for the 100 Ω standard.

Figure 3 shows the initial precision measurements at the beginning, when all samples have comparable carrier densities $1–2 \times 10^{11}$ cm^{-2}. Figure 3(a) shows an example of a CCC-measurement campaign, where one epigraphene QHR was compared to 100 Ω. The measurement assumes that the QHR has an exact resistance value of $h/(2e^2)$, where h is the Planck constant. The CCC will then provide a measure of the relative deviation of the 100 Ω standard from its nominal value of 100 Ω. Each point represents a measurement series
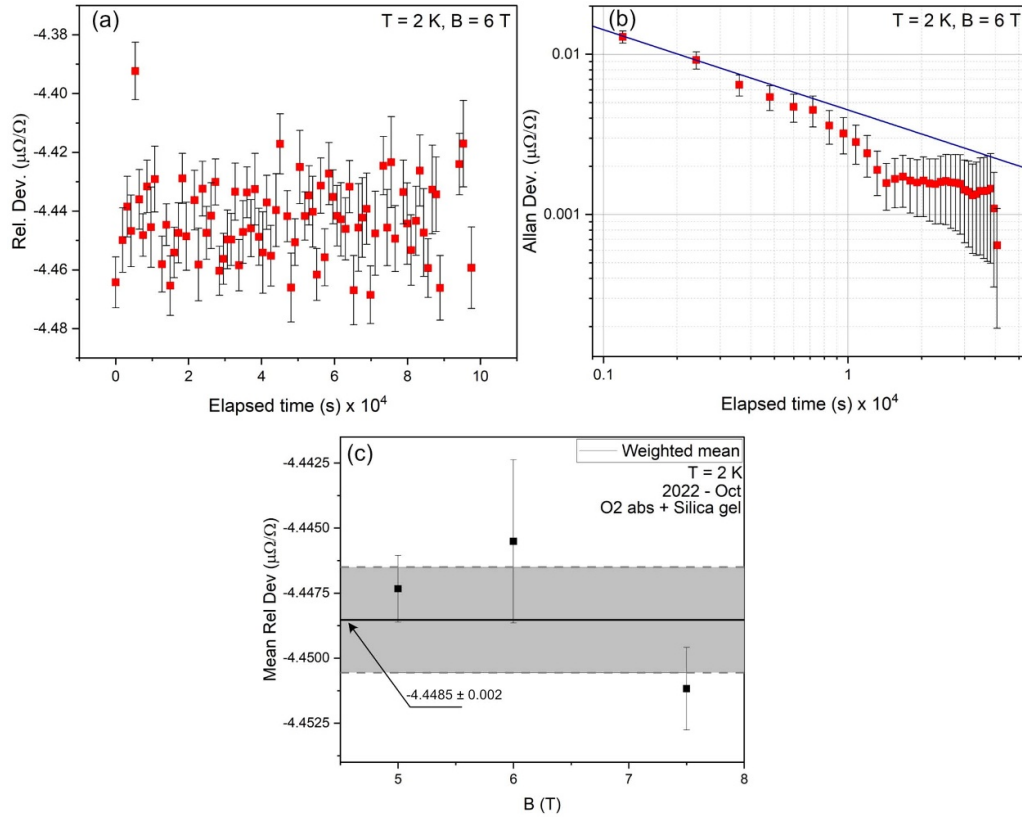
Figure 4. (a) Precision cryogenic current comparator (CCC) measurement taken for one of the stable samples (Atecom) kept for 700 d in the mixer of O_2 absorber + silica gel versus standard resistor with nominal value of 100 Ω, which shows their relative deviation at $B = 6$ T and $T = 2$ K. (b) Allan deviation follows $1/t^{1/2}$ (blue line), which indicates that white noise dominates and limits the measurement uncertainty to 1 $\mu\Omega\ \Omega^{-1}$. (c) shows mean relative deviation between sample and 100 Ω standard resistor. The grey shaded area is the one standard deviation from the weighted mean (black line) of all data points.

of roughly 15 min, which includes polarity switches to cancel thermal voltages. The error bars represent one standard deviation. From this data the weighted mean is calculated, which is $-4.4674\ \mu\Omega\ \Omega^{-1}$ with standard deviation of weighted mean of $0.0041\ \mu\Omega\ \Omega^{-1}$. The exact calculations are described in related works [14]. Figure 3(b) shows the corresponding Allan deviation analysis [20] (using overlapping Allan deviation as in [14]). The blue line is a fit to $1/t^{1/2}$, where t is elapsed measurement time. This line indicates pure white noise behavior, and we can see that white noise dominates down to below 1 $n\Omega\ \Omega^{-1}$, which is an acceptable uncertainty limit for quantum resistance metrology.

Figures 3(c) and (d) shows a summary of comparison measurements for the four of each Atecom and Cree chips respectively, derived from data like in (a). Each point is the weighted mean relative deviation of the 100 Ω standard from its nominal value, and each error bar is the standard deviation of the weighted mean, limited by Allan deviation for each measurement campaign (at 10^4 s). All the points agree with each other within the expanded type A uncertainty. This supports the fact that all eight samples are quantized. The black line represents the weighed mean of the chips, and the grey zone represents one standard deviation of the weighted mean. The corresponding values are shown in the figures with arrow pointing to the line corresponding to the weighted mean.

Note that the slight difference in weighted mean values of the relative deviation of the 100 Ω standard when measured via Atecom or Cree is within the expected drift and short-term instability of the 100 Ω over two months (see figure 5).

6. Effects of long-term storage on quantization

Figure 4 shows precision measurements for one of the samples kept in the most stable environment: desiccant/oxygen absorber mixture.

While these samples showed very low drift in carrier density over time, we also wanted to rule out the possibility that the sample has degraded in other ways. We performed a new set of precision measurements after an extended storage period, again using the stable 100 Ω standard, to verify that no detrimental changes occurred in the sample which spoils quantization accuracy (e.g. increased charge inhomogeneity).

Precision measurements taken at three different magnetic fields show that the sample is well-quantized. The weighted mean and standard deviation of weighted mean is $(-4.4485 \pm 0.0020)\ \mu\Omega\ \Omega^{-1}$. The relative deviation from this set of measurements is also in good agreement with the value of the 100 Ω standard when compared to other QHRs (see figure 5). We can conclude that there is
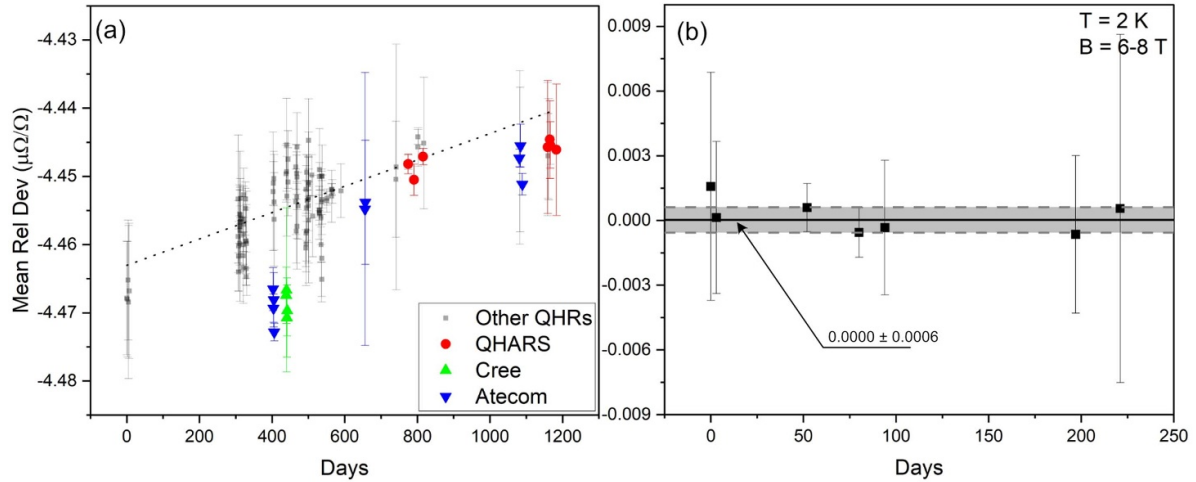
Figure 5. (a) Precision CCC measurement of 100 Ω resistance standard compared against various standards. The comparison measurements were formed against various graphene quantum Hall resistance (QHR) standards ('Other QHR'), quantum Hall array resistance standard (QHARS), and the Cree and Atecom samples described in this work. Slope of the mean relative deviation between 100 Ω standard compared to various QHRs over three years indicate that the drift in the 100 Ω resistor is on the order of 2 nΩ Ω^{-1} per 100 d. The error bars represent one standard deviation. (b) shows the direct comparison precision measurements between graphene quantum Hall arrays stored in desiccant/oxygen absorber environment. The grey shaded area is one standard deviation from the weighted mean (black line) of all data points. The mean relative deviation between the QHARSsis within 0.03 nΩ Ω^{-1} with an uncertainty of 0.6 nΩ Ω^{-1}.

no detrimental long-term effect of sample storage in desiccant/oxygen absorber mixture thus far.

Note that the other storage techniques such as oxygen absorber or ambient resulted in significant drift of carrier density and those samples can no longer be measured under standard operating conditions in our laboratory. The carrier density was either too low to allow for sufficiently high bias currents (at least 23 μA), or too high for operation below 12 T (maximum field of our magnet).

Figure 5(a) shows a summary of numerous precision comparison measurements between the 100 Ω standard and various graphene QHRs taken over approximately 3 years. The black data represent comparison measurements between the 100 Ω standard and QHRs not discussed in this work (roughly 10 samples total, similar to those described in [11]). The green and blue data are the Cree and Atecom samples respectively. In general, all measurements follow the slow linear long-term drift of the 100 Ω standard of approximately 2 nΩ Ω^{-1} per 100 d. The short-term stability (e.g. due to temperature and pressure fluctuations) of the standard can be significantly worse and is included as noise in the measurements, giving a typical standard deviation of up to 10 nΩ Ω^{-1} for the mean relative deviation from nominal value. The inherent instability of the 100 Ω limits the ultimate precision with which we can compare the quantization for Cree and Atecom samples, and how it develops over time.

As a final test we have also employed the recently developed graphene quantum Hall array resistance standard (QHARS) [14], with array resistance close to 109 Ω and consisting of 236 connected Hall bars. These arrays were stored in a similar desiccant/oxygen absorber environment and allow for more precise comparison measurements to 100 Ω standard

(red data in figure 5(a)), which provides additional support for the long-term stability of the quantization accuracy of the sample stored in the mixed desiccator/oxygen absorber environment. Furthermore, the arrays were also used to perform direct comparisons between quantum standards. The group of data attributed to 'Other QHRs' represent comparison measurements of the 100 Ω standard against various QHRs not explicitly mentioned in this work. They are also not all stored in a controlled environment. This data set allows us to observe the long-term drift of the 100 Ω standard. Figure 5(b) shows the direct comparison measurement between two QHARSs (on the same chip) after long-term storage in mixed environment. Due to the direct comparison between arrays with 1:1 ratio, the noise in this type of measurement is very low, and the uncertainty can approach 0.1 nΩ Ω^{-1} with sufficient averaging [14]. The resistance value of the QHARSs also have no inherent drift, so any discrepancy in quantization can be attributed to sample degradation. The data shows that the relative deviation between the QHARSs is zero within the noise level of 0.6 nΩ Ω^{-1} for over 225 d and counting. We can therefore conclude that there is no discernable degradation of the quantization accuracy at the sub part-per-billion level for samples stored in oxygen absorber and desiccant mixture.

7. Discussion

Our observations reveal that ambient exposure induces large amounts of p-doping to the samples (all our samples start out as n-doped), consistent with existing reports in literature [12]. Moisture from ambient is one key contributor to p-doping. The result is that after 700 d all samples kept in ambient are close to

the charge neutrality point and unsuitable for use in precision measurements.

The desiccant removes moisture, it is therefore expected that stability should improve. We do observe increased stability compared to ambient, but with some noticeable drift still, and with some volatility in the carrier density. We attribute this behavior to imperfect sealing of the bottles (i.e. leakage), as the trend in general is still that p-doping increases over time. The samples could survive for an extended period, but the volatility in carrier density is undesirable. The bottle and caps used in this work have no special seals or linings, which leaves room for future improvement.

Storage in oxygen absorber yields opposite results, with an extremely strong n-doping effect over time. The samples quickly become unviable for QHR measurements due to high n-doping levels. Our samples are encapsulated with polymer and uses molecular dopants F4TCNQ to p-dope epigraphene. The exact interaction between polymer, dopant molecules, and oxygen absorber are complicated and unknown to us at this point. Note that the p-doping effect that iron has on graphene is known [21], and the F4TCNQ-molecules strongly interact with metals [13]. The observed n-doping could be that the efficacy of F4TCNQ is reduced due interference from iron particles and/or the iron particles provide strong doping by themselves. Both the chip and sample holder have a noticeable red hue after long-term storage, indicating the adsorption of rust particles on all surfaces. While the exact mechanism of n-doping from oxygen absorber needs further investigation, the doping effect is extremely prominent, with 500%–600% increase in n-type carriers after 700 d. This is by itself an interesting observation and could be leveraged for carrier density control in the future.

The oxygen absorber mixed with desiccant provided the most consistent and stable storage environment. The strong n-doping effect of the oxygen absorber is clearly being suppressed by the desiccant. We employ a food-grade oxygen absorber which relies on moisture to function. The oxygen absorber sachets already have water in them to aid in this reaction. The presence of desiccants removes most of this water which greatly slows down the formation of iron oxides, the likely culprit behind the strong n-doping. We know that a significant amount of water is being absorbed by the desiccants since they get saturated and turn white immediately in the presence of the oxygen absorber sachets (see figure 1, fourth bottle). Contrast this to the pure desiccant bottle, which retains the yellow color even after 700 d due to the limited amount of available moisture.

Due to the saturation of desiccant beads, the oxygen absorber could still have some moisture remaining. It could also receive additional moisture from leaks in the bottle caps and/or when the bottles are opened to retrieve the samples. Whatever small amount of moisture is left, it is enough to activate the oxygen absorber and provide a weak n-doping effect which compensates the slow p-doping effect seen in storage in pure desiccant environments. The optimal ratio between desiccant and oxygen absorber needs to be investigated in future work.

We have tried two different ratios of desiccant and oxygen absorber. The one discussed above and shown in figure 1, and another larger bottle with the ratio of desiccants to oxygen absorber increased two-fold (QHARSs were stored in this). All the beads in the bottle with increased desiccant content are still orange, which means that they have not been saturated. We speculate that even if the desiccant removes all the initial moisture from the oxygen absorbers, whatever extra moisture is introduced via leaks or when opening the bottle activates the oxygen absorber again. This n-doping effect automatically compensates the p-doping effect of the increased moisture, leading to the long-term stability in carrier density that we observe. The challenge in controlling the stability of the QHARS is that any minor deviation in device homogeneity of any individual Hall bar out of 236 will be detrimental to the final array accuracy. However, the precision measurements reveal that the QHARSsamples show excellent long-term stability, which proves the efficacy of the storage technique for all 236 Hall bars.

From the drift of carrier densities we also observed that the Atecom samples are more stable compared to Cree in general. We indirectly observed this during the fabrication step. Due to the difference in substrate types, the initial doping levels are likely different for the samples. Although all samples used the same molecular dopant method [11, 13], it took different thermal annealing times to reach comparable carrier densities of 1–2 cm^{-2} $\times$ 10^{11} cm^{-2} (n-type). The Atecom samples experienced twice the annealing time compared to Cree. We have previously observed that extended annealing can improve stability of molecular doped samples [22], and the stability of Atecom samples could be due to a related phenomenon. However, extended thermal annealing would historically remove most of the p-doping effect of molecular dopants, which is not the case for Atecom samples. We observe that the samples are difficult to thermally anneal to higher n-doping levels, indicative of high stability of dopants. The interaction between vanadium doped SiC substrates and molecular dopants warrants further investigations to understand the nature of increased doping stability. More studies are also needed to investigate the advantages of vanadium doped substrates for more stable graphene devices.

8. Conclusion

In this paper, we studied four different inexpensive storage solutions and their influence on transport properties of polymer encapsulated molecular doped graphene over 700 d. We have found that mixture of oxygen absorber and desiccant provides reliable, and highly stable storage solution for the epitaxial graphene QHRs, which can be easily incorporated in any situation which requires low maintenance and long-term stability of the sample. The stability is comparable to the current state-of-the-art storage techniques which use nitrogen atmosphere. The proposed storage method using desiccant/oxygen absorber mixture in a sealed glass bottle offers a simple and practical alternative which is widely available.

Further studies are required to understand the nature of reaction between the storage chemicals, molecular dopants, and substrate type to fully understand the principles behind the stability of the electronic properties of graphene devices. Such investigations would aid in the optimization of simple storage techniques and allow for graphene QHR standards to reach long-term stabilities comparable to GaAs-based systems.

Acknowledgments

ORCID iDs

Naveen Shetty ● https://orcid.org/0000-0002-1230-7048
Tobias Bergsten ● https://orcid.org/0000-0003-2330-9898
Samuel Lara Avila ● https://orcid.org/0000-0002-8331-718X
Sergey Kubatkin ● https://orcid.org/0000-0001-8551-9247

References

[1] Tzalenchuk A *et al* 2010 Towards a quantum resistance standard based on epitaxial graphene *Nat. Nanotechnol.* **5** 186–9

[2] Ribeiro-Palau R *et al* 2015 Quantum Hall resistance standard in graphene devices under relaxed experimental conditions *Nat. Nanotechnol.* **10** 965–71

[3] Janssen T J B M *et al* 2011 Graphene, universality of the quantum Hall effect and redefinition of the SI system *New J. Phys.* **13** 093026

[4] Schopfer F and Poirier W 2013 Quantum resistance standard accuracy close to the zero-dissipation state *J. Appl. Phys.* **114** 064508

[5] Chatterjee A *et al* 2023 Performance and stability assessment of graphene-based quantum Hall devices for resistance metrology *IEEE Trans. Instrum. Meas.* **72** 1502206

[6] Chae D-H *et al* 2022 Investigation of the stability of graphene devices for quantum resistance metrology at direct and alternating current *Meas. Sci. Technol.* **33** 065012

[7] Novoselov K S, Geim A K, Morozov S V, Jiang D, Katsnelson M I, Grigorieva I V, Dubonos S V and Firsov A A 2005 Two-dimensional gas of massless Dirac fermions in graphene *Nature* **438** 197–200

[8] Kopylov S, Tzalenchuk A, Kubatkin S and Fal'ko V I 2010 Charge transfer between epitaxial graphene and silicon carbide *Appl. Phys. Lett.* **97** 112109

[9] Janssen T J B M, Rozhko S, Antonov I, Tzalenchuk A, Williams J M, Melhem Z, He H, Lara-Avila S, Kubatkin S and Yakimova R 2015 Operation of graphene quantum Hall resistance standard in a cryogen-free table-top system *2D Mater.* **2** 035015

[10] Alexander-Webber J A *et al* 2016 Giant quantum Hall plateaus generated by charge transfer in epitaxial graphene *Sci. Rep.* **6** 30296

[11] He H *et al* 2019 Polymer-encapsulated molecular doped epigraphene for quantum resistance metrology *Metrologia* **56** 045004

[12] Panchal V, Giusca C E, Lartsev A, Martin N A, Cassidy N, Myers-Ward R L, Gaskill D K and Kazakova O 2016 Atmospheric doping effects in epitaxial graphene: correlation of local and global electrical studies *2D Mater.* **3** 015006

[13] He H *et al* 2018 Uniform doping of graphene close to the Dirac point by polymer-assisted assembly of molecular dopants *Nat. Commun.* **9** 3956

[14] He H, Cedergren K, Shetty N, Lara-Avila S, Kubatkin S, Bergsten T and Eklund G 2022 Accurate graphene quantum Hall arrays for the new international system of units *Nat. Commun.* **13** 1–9

[15] Park J, Lim K-G and Chae D-H 2022 Glass encapsulation of molecular-doped epitaxial graphene for quantum resistance metrology *Meas. Sci. Technol.* **33** 115019

[16] Cichello S A 2015 Oxygen absorbers in food preservation: a review *J. Food Sci. Technol.* **52** 1889–95

[17] Shetty N *et al* 2023 Scalable fabrication of edge contacts to 2D materials: implications for quantum resistance metrology and 2D electronics *ACS Appl. Nano Mater.* **6** 6292–8

[18] Delahaye F and Jeckelmann B 2003 Revised technical guidelines for reliable dc measurements of the quantized Hall resistance *Metrologia* **40** 217–23

[19] Yager T *et al* 2015 Low contact resistance in epitaxial graphene devices for quantum metrology *AIP Adv.* **5** 87134

[20] Allan D W 1987 Should the classical variance be used as a basic measure in standards metrology? *IEEE Trans. Instrum. Meas.* **IM–36** 646–54

[21] Pi K, McCreary K M, Bao W, Han W, Chiang Y F, Li Y, Tsai S-W, Lau C N and Kawakami R K 2009 Electronic doping and scattering by transition metals on graphene *Phys. Rev.* B **80** 1–5

[22] He H, Shetty N, Bauch T, Kubatkin S, Kaufmann T, Cornils M, Yakimova R and Lara-Avila S 2020 The performance limits of epigraphene Hall sensors doped across the Dirac point *Appl. Phys. Lett.* **116** 223504